

1N-14
110073
p. 26

Design Characteristics of a Heat Pipe Test Chamber

Karl W. Baker
National Aeronautics and Space Administration
Lewis Research Center
Cleveland, Ohio

J. Hoon Jang
Sverdrup Technology, Inc.
Lewis Research Center Group
Brook Park, Ohio

and

Juin S. Yu
West Virginia Institute of Technology
Montgomery, West Virginia

Prepared for the
First International Conference on Aerospace Heat Exchanger Technology
cosponsored by the ASME and AIAA
Palo Alto, California, February 15-17, 1993



DESIGN CHARACTERISTICS OF A HEAT PIPE TEST CHAMBER

Karl W. Baker

NASA Lewis Research Center, Cleveland, Ohio 44135

J. Hoon Jang

Sverdrup Technology, Inc., NASA Lewis Research Group, Cleveland, Ohio 44135

Juin S. Yu

West Virginia Institute of Technology, Montgomery, West Virginia 25136

ABSTRACT

The Lewis Research Center of the National Aeronautics and Space Administration has designed a heat pipe test facility which will be used to provide data for validating heat pipe computer codes. A heat pipe test chamber that uses helium gas for enhancing heat transfer has been investigated. The conceptual design employs the technique of guarded heating and guarded cooling to facilitate accurate measurements of heat transfer rates to the evaporator and from the condenser. The design parameters are selected for a baseline heat pipe made of stainless steel with an inner diameter of 38.10 mm and a wall thickness of 1.016 mm. The heat pipe operates at a design temperature of 1000 K with an evaporator radial heat flux of 53 W/cm².

INTRODUCTION

The Lewis Research Center has designed a heat pipe test facility which will be used to provide data for validating heat pipe computer codes. The apparatus has the capability of operating heat pipes at heat loads up to 20 kW with a radial heat flux of 53 W/cm². These large heat loads are necessary to experimentally define boiling and capillary limits for a variety of heat pipes including high performance liquid metal heat pipes. The heat pipe operating temperatures of interest in this work fall within the range from 400 to 1000 K. An additional requirement is to measure heat flows and temperatures as accurately as possible for code validation purposes.

Testing heat pipes with high heat fluxes in a vacuum environment where heat transfer takes place only by radiation requires excessively high heating element temperatures. A temperature of approximately 2400 K at a radial heat flux of 50 W/cm² will result in conditions where undesirable effects such as thermal/chemical instability of the heater material, loss of structural integrity due to creep, and possible catastrophic damage to the

heater due to thermal shock may occur. Induction heating was considered, but was ruled out for several reasons; the most important reason being the problem of measuring heat input and temperatures under the heating element.

A heat pipe test chamber featuring the presence of helium gas has been investigated. Helium, which is thermally stable, has a high thermal diffusivity, is chemically inert and has a thermal conductivity close to that of hydrogen, is used to increase heat transfer by conduction. With the addition of this gas, the overall heat transfer process can be improved such that the temperature of the heating element can be reduced to tolerable levels (below 1900 K) and heat extraction rates from the condenser are also improved to acceptable levels (32 W/cm² of radial heat flux). The major emphasis of this study has been placed on determining system requirements and developing design parameters for the construction of a laboratory test apparatus that can test cylindrical heat pipes at operating temperatures up to approximately 1000 K with a radial heat flux of roughly 53 W/cm² using electrical resistance heating.

DESCRIPTION OF SYSTEM COMPONENTS

The design of the helium filled test chamber is schematically illustrated in Fig. 1. The heat pipe evaporator, adiabatic, and the condenser sections are shown. The helium

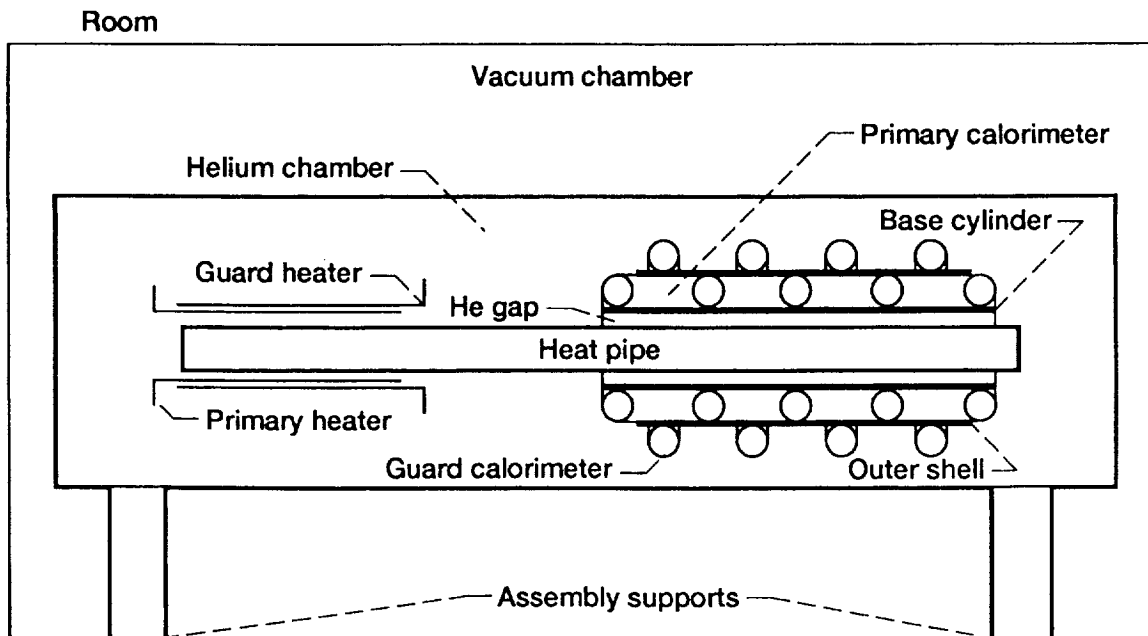


Figure 1.—Schematic arrangement of system components.

chamber is placed inside a large vacuum chamber. The heat pipe, heaters, and calorimeters are housed within the closed walls of the helium chamber. The operation of the system calls for the use of guarded heating and guarded cooling techniques to accurately determine the heat transfer rates to the evaporator and from the condenser of the heat pipe. The heating assembly is made up of two thin-walled concentric heaters, each having a thickness of 0.157 cm. The inner or primary heater is used to supply heat to the heat pipe over the evaporator section while the outer or guard heater is intended exclusively to

minimize the heat flow between the two heaters by operating at the same temperature as the primary heater. The cooling unit is held coaxially over the condenser section of the heat pipe and is comprised of two concentric spiral flow channels, each being a transversely closed flow path integrated to a thin-walled cylinder. The inner channel, or the primary calorimeter, transfers the heat output of the condenser to a coolant flow. A separate coolant flow of identical temperature flows through the outer channel, the guard calorimeter, which is intended to minimize any radial heat flow between the two calorimeters. A baseline heat pipe having the physical dimensions specified in Table I is employed in an analysis for the selection of system parameters. The nominal design operating requirements are also presented in the table. The containment envelope of the heat pipe, the helium chamber, and the vacuum chamber are all made of AISI 304 stainless steel.

Table I.—Baseline heat pipe dimensions and nominal design requirements.

Baseline heat pipe at room temperature: (Dimensions in cm)	
Inside diameter	3.81
Wall thickness	0.102
Overall length	100
Evaporator length	30
Adiabatic length	20
Condenser length	50
Nominal design requirements:	
Heat pipe temperature, K	1000
Maximum heater temperature, K	1900
Evaporator heat load, kW _{th}	20
Helium chamber wall temperature, K	1000

Heater Assembly

A cutaway representation of the heater section at the evaporator of the heat pipe is shown in Fig. 2. All the components shown in the sketch are cylindrical in form and concentric about the heat pipe axis. Table II presents the thicknesses of the various components. Helium gas, initially at atmospheric temperature and pressure, fills any void space inside the test chamber. The primary and guard heaters, have the same thickness but differ in diameter, with the guard heater being larger. Each heater is comprised of two layers of pyrolytic boron nitride (PBN) with a thin layer of pyrolytic graphite (PG) heating element imbedded in between.

● Thermocouples

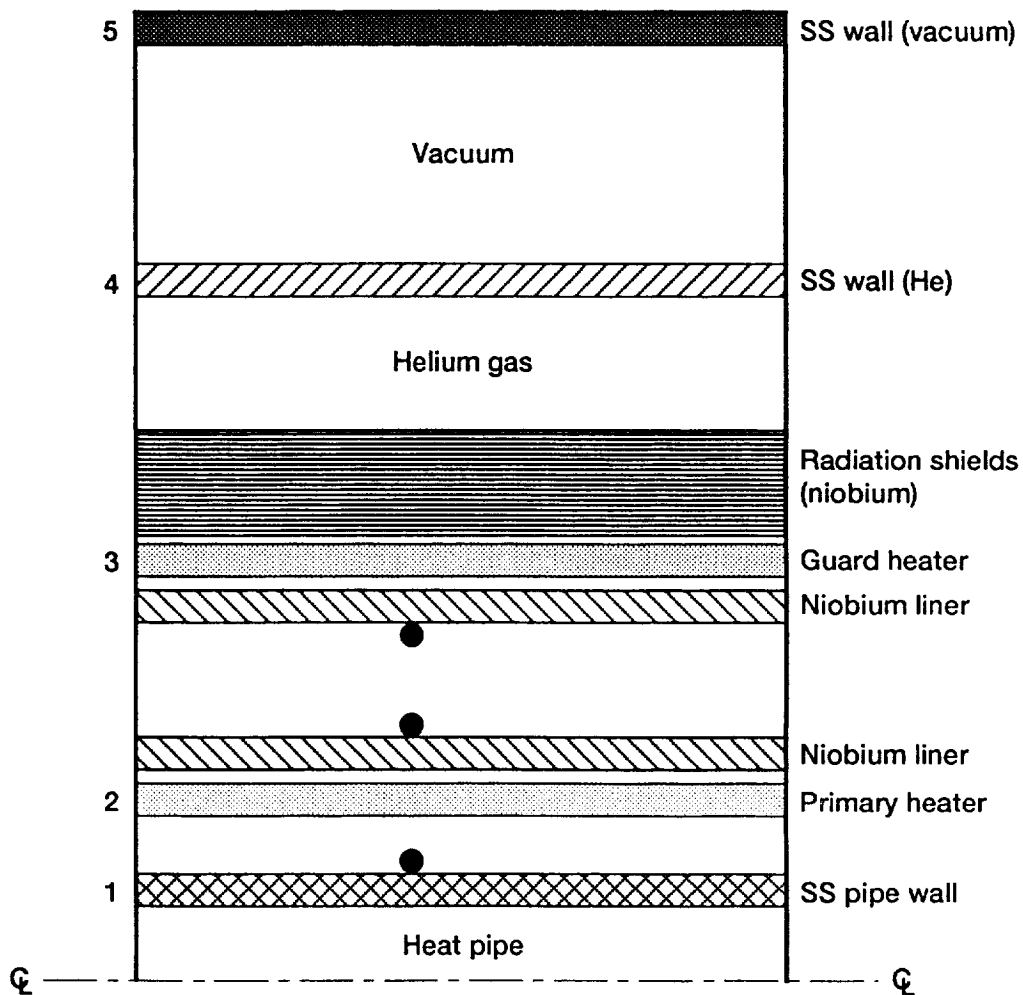


Figure 2.—Structure detail of heater assembly; numbers serve as component labels.

Table II.—Heater assembly component layer thickness at room temperature.

(All dimensions in mm.)

PBN/PG resistance heaters . . .	1.575
Niobium liners	0.5
Niobium radiation shields	0.025
Niobium wire screen (mesh 4/in.)	0.5
SS wall of helium chamber . . .	6.350
SS wall of vacuum chamber . .	7.9375

A cutaway view across the thickness of a typical heating element is shown in Fig. 3. These heaters are capable of operating at temperatures up to 2300 K which gives a comfortable operating margin at the maximum design temperature of 1900 K. A guard

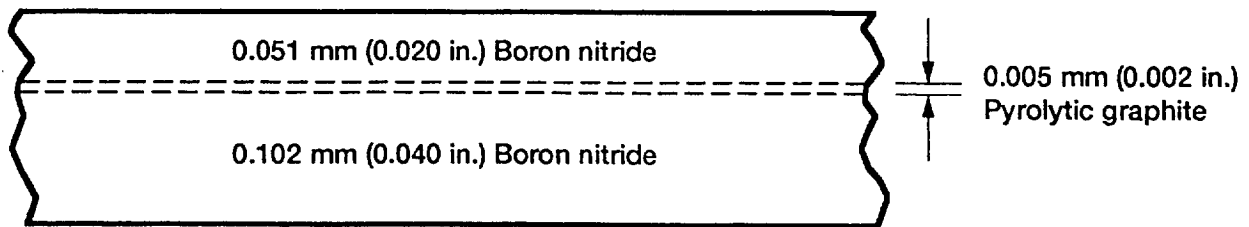


Figure 3.—Structure of boron nitride/pyrolytic graphite resistance heater.

heater is used to effectively eliminate the flow of heat radially outward from the primary heater. With the guard heater operating at the same temperature as the primary heater the electrical power input to the primary heater is equal to the input thermal power to the evaporator of the heat pipe, neglecting some minor heat losses. To facilitate heater temperature measurement two niobium liners are installed between the primary and guard heaters, as shown in Fig. 2. This was done to avoid attaching metallic thermocouples directly to the boron nitride coating of the heater element, which according to the heater manufacturer would be difficult if not impossible. Each liner is instrumented with thermocouples and the power to the guard heater is controlled so that the liners are always at the same temperature. Multiple layers of radiation shields and supporting wire screen, both made of niobium to withstand high temperatures, are used to suppress the radially outward flow of heat from the guard heater. This reduces electrical power requirements for the guard heater as well as reduces the temperature of the helium chamber. Because of this temperature reduction a stainless steel wall could be used instead of more expensive niobium. The apparatus was designed so the helium chamber wall is always below 1000 K to meet mechanical strength requirements.

One of the major drawbacks to radiation heating for this application is that the input heat to the heat pipe cannot be shut off abruptly. The electrical power input to the heater can be shut off but residual heat from the heater assembly will continue to flow into the heat pipe. This effect can destroy heat pipes if dry-out is experienced. At the dry-out condition the heat pipe wick structure will cease to pump liquid back to the evaporator, decreasing the effective thermal conductivity of the heat pipe by several orders of magnitude. This condition can be quickly detected by thermocouples mounted on the heat pipe and the heater power can be shut off immediately. Since the heat pipe can no longer transfer heat effectively, the residual heat stored in the heater assembly will flow into the heat pipe, increasing its temperature. The resulting temperature could be over the melting temperature of the containment envelope material of the heat pipe in the evaporator section. Therefore, it is desired to minimize the amount of residual heat stored in the heater assembly. This is rather difficult to do since the specific heat of boron nitride is approximately seven times greater than stainless steel.

Two methods have been devised to circumvent the problem of residual heat storage in the heater causing heat pipe destruction on dry-out. First, when an over temperature is sensed on the evaporator surface of the heat pipe, a safety switch will terminate power to the heater and the heat pipe will be automatically tilted so that gravity will aid in returning fluid to the evaporator. The returning fluid will transfer the residual heat from the heating element and prevent the containment envelope from melting. A second solution being considered is to install a nozzle near the heater assembly and inject cool helium gas on the heater and heat pipe when an over temperature is sensed.

Primary Heater

The primary heater is used to supply heat to the evaporator section of the heat pipe. The helium gap between the heat pipe and the primary heater is critical and must be sized to meet heat transfer requirements at operating conditions (see Table I).

It is assumed that end effects are small and axial conduction through the helium gas and the heater wall may be ignored. As a good approximation, the heater shell may be assumed to generate heat uniformly throughout. Because of the small gap between the heater and the heat pipe free convection of the helium gas was shown, by using standard formulae (Incropera & Dewitt, 1990), to contribute very little to the heat transfer between the primary heater and the heat pipe and was therefore neglected. Using the component Tables introduced in Fig. 2, the steady state radial heat flow equations are as follows:

To account for heat conduction across the stainless steel heat pipe wall

$$Q_{ph} = 2\pi k_1 l_e (T_{o1} - T_{i1}) / \ln \frac{d_{o1}}{d_{i1}} \quad (1)$$

To account for radiation and conduction across the helium gap

$$Q_{ph} = l_e \left[\frac{\pi \sigma d_{o1} (T_{i2}^4 - T_{o1}^4)}{\epsilon_{o1}^{-1} + (\epsilon_{i2}^{-1} - 1) d_{o1} / d_{i2}} + \frac{2\pi k_{he} (T_{i2} - T_{o1})}{\ln(d_{i2} / d_{o1})} \right] \quad (2)$$

To account for conduction across the pyrolytic graph graphite/boron nitride heater

$$Q_{ph} = 4\pi k_2 l_e \left(1 - \frac{d_{i2}^2}{d_{o2}^2} \right) (T_{o2} - T_{i2}) / \left(\frac{d_{i2}^2}{d_{o2}^2} - 1 - 2 \ln \frac{d_{i2}}{d_{o2}} \right) \quad (3)$$

where d_{ij} is the inside diameter of component j , and

$$d_{oj} = d_{ij} + 2\delta_j, \quad \text{where } j = 1, 2, \dots, n - 1; n = \geq 2 \quad (4)$$

and $j = 1, 2, \dots, n - 1; n \geq 2$ is the outside diameter, with δ_j being the thickness. The heater has uniform heat generation everywhere and an insulated boundary at the outer surface.

Equations (1) to (3) are employed, in conjunction with Eq. (4), to compute the temperatures T_{o1} , T_{i2} , and T_{o2} . The baseline heat pipe inside diameter (d_{i1}) was used with the design value of the primary heater power output (Q_{ph}) for this computation. Also the heat

pipe operating temperature was assumed to be (T_{ii}). Temperature variations of thermo-physical properties of air and helium were accounted for with data from Incropera & DeWitt (1990), from Touloukian & Ho (1972), for niobium and SS304, and the emissivity of stainless steel was given by Banks et al. (1988). Data published by the Union Carbide Coating Service Corp (1990) for the pyrolytic graphite/boron nitride heaters was also used. Material properties not readily available at high temperatures were estimated by extrapolation. In the above equations, the thermal conductivities and the component thicknesses were determined at their respective average temperatures; all other quantities were evaluated at the prevailing local temperatures except the active working length of the primary heater. Thermal expansion causes the pyrolytic graphite/boron nitride heater elements to undergo little change in the axial direction, therefore the length of the heater is set equal to the length of the evaporator section (L_p) of the heat pipe.

A graphical presentation of the calculated gap sizes are shown in Fig. 4 where, for the design evaporator heat load of $Q_{ph} = 20$ kW, the required working size of the helium gap

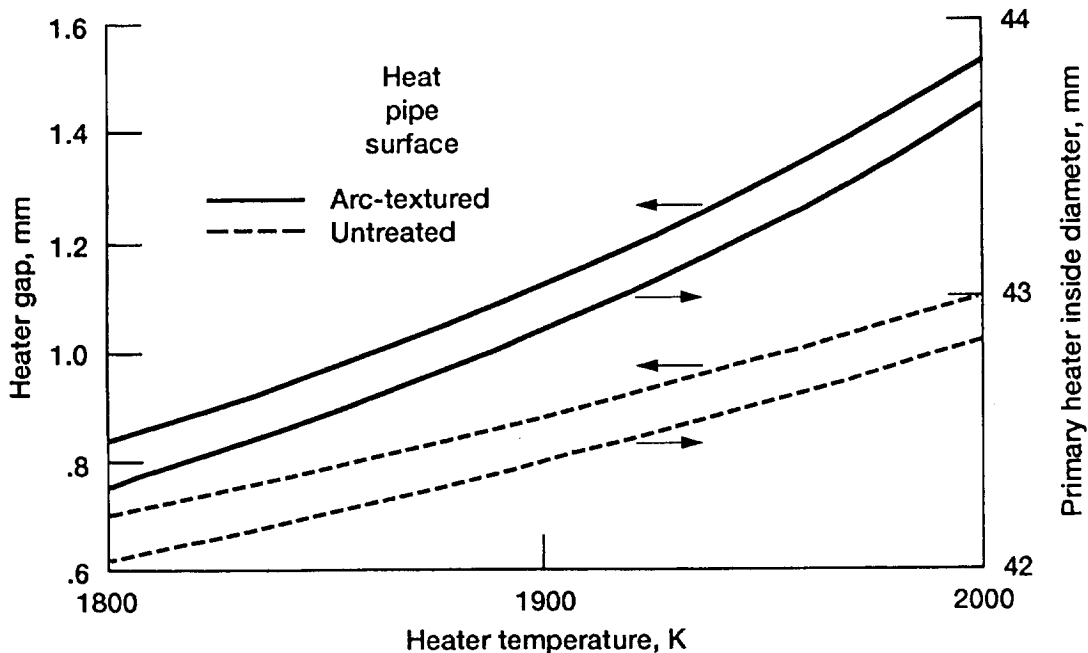


Figure 4.—Primary heater requirements at operating conditions.

at operating temperature is given as a function of the primary heater temperature. Also shown is the value of the heater inside diameter. The diameter of the primary heater is measured at room temperature. Two cases are considered for the sake of comparison. The solid lines represent a heat pipe with an arc-textured evaporator surface while the dashed lines are the results if the heat pipe surface is untreated. With a heater temperature at $T_{02} = 1900$ K, the operating gaps for the two respective cases must be 1.12 and 0.88 mm in order to transfer 20 kW of heat into the heat pipe evaporator. Though the use of a larger gap retards heat conduction, arc-texturing the heat pipe surface greatly improves the emissivity of the surface and therefore significantly increases the rate of heat transfer by radiation, especially at heater temperatures above 1100 K. A larger gap is desired for clearance of thermocouple wires as well as ease of fabrication. The final balancing between the two opposing effects, subject to meeting the required design

conditions yields a significantly larger gap which is highly desired from the viewpoint of system fabrication. It should be noted here that Eq. (3), which relates to the heater surface temperatures, is obtained by assuming uniform heat generation within the entire solid body of the primary heater. More accurate heater surface temperatures have been computed by confining the internal heat generation within the region of the graphite heating element (see Fig. 3). The latter procedures are not presented because the formulation is mathematically tedious and the computation time consuming. The overall result indicates a reduction of less than 10 percent in the size of the helium gap from those shown in Fig. 4 at the same heater temperature, e.g., 1.03 versus 1.12 mm with an arc-textured heat pipe and 0.83 versus 0.88 mm with pipe untreated, both with a heater surface temperature of 1900 K.

The ratio of heat transferred from the primary heater to the heat pipe by conduction to that by radiation, versus heater temperature, is given in Fig. 5. More heat is transferred

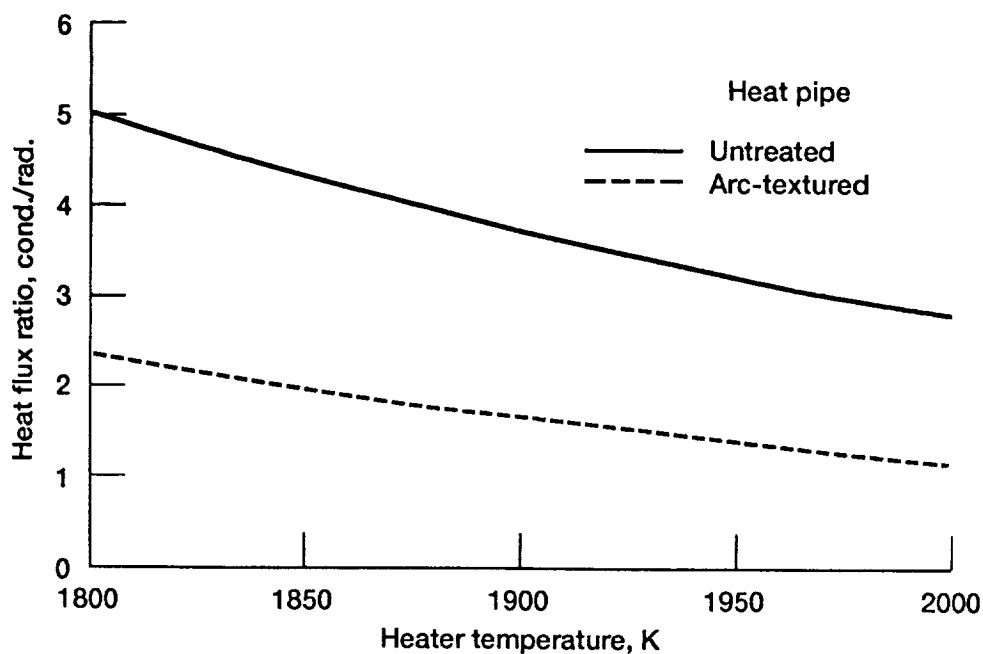


Figure 5.—Radial heat flux ratio versus primary heater temperature.

by conduction than radiation up to $T_{ph} = 2000$ K where the ratio almost equals unity for the arc-textured case. For the untreated case, conduction heat transfer dominates by a much larger margin as shown, with a heat flux ratio of 5.0 with $T_{ph} = 1800$ K.

Guard Heater

It is desirable to operate the guard heater unit with a minimal heat output and to maintain the wall temperature of the stainless steel helium chamber at less than 1000 K. The use of radiation type shields within the helium environment reduces both the power requirement and the helium chamber wall temperature. However, adding shields has diminishing returns as the number of layers increases beyond some point. To provide an estimate for the number of shields it is necessary to proceed through the pertinent heat

flow equations, from the guard heater itself to the room air outside of the vacuum chamber and the surrounding walls of the room. Only radial heat flow is considered and the necessary equations are established on the assumption that the rate of heat generated in the guard heater can be equated to the rate of heat transfer to the surrounding room via the intermediate components which are treated as long isothermal cylinders. The use of such an approximation tends to overestimate both the heat flow and the stainless steel helium chamber wall temperatures. However, this analysis is intended to provide a reliable conservative estimate of the guard heater design requirements.

The heat generation is treated as being uniformly distributed throughout the boron nitride shell as before. Subscriptive notations depicted in Fig. 2 are used for referencing the various component sections. The guard heater, in operation, is essentially insulated at the inner boundary. The guard heating element surface temperatures are related by the conduction heat flow equation

$$Q_{gh} = 4\pi k_3 l_e \left(\frac{d_{o3}^2}{d_{i3}^2} - 1 \right) (T_{i3} - T_{o3}) / \left(\frac{d_{o3}^2}{d_{i3}^2} - 1 - 2 \ln \frac{d_{o3}}{d_{i3}} \right) \quad (5)$$

In the absence of heat shields, the space between the guard heater and the helium chamber wall is approximated as an enclosure formed by two concentric cylinders of equal length with the annulus open at both ends to background radiation from the surrounding helium chamber. The heat exchange due to radiation heat transfer was accounted for and calculations are shown in Appendix. The total heat flow from the guard heater due to combined conduction and radiation satisfies the equation

$$Q_{gh} = \frac{2\pi l_e k_{he} (T_{o3} - T_{i4})}{\ln(d_{i4}/d_{o3})} + Q_{o3}(T_{o3}, T_{o4}, T_{o4}) \quad (6a)$$

The net rate of heat transfer to the portion of the helium chamber wall equal in length to that of the guard heater is

$$Q_4 = \frac{2\pi l_e k_{he} (T_{o3} - T_{i4})}{\ln(d_{i4}/D_{o3})} - Q_{o4}(T_{o3}, T_{o4}, T_{o4}), \quad (6b)$$

k_{he} is the thermal conductivity of the helium gas at the mean temperature between T_{o3} and T_{i4} . Q_{o3} and Q_{o4} are functions of the indicated surface temperatures as formulated in the Appendix.

With radiations shields used over the guard heater, the approximation of long concentric cylinders may be applied to describe the radial heat flow up to the outermost radiation shield. Between the guard heater and the first radiation shield

$$Q_{gh} = \left[\frac{\pi \sigma d_{o3} (T_{o3}^4 - T_{r1}^4)}{\epsilon_{o3}^{-1} + (\epsilon_{r1}^{-1} - 1) d_{o3} / d_{r1}} + \frac{2\pi k_{eff}^{(1)} (T_{o3} - T_{r1})}{\ln(d_{r1} / d_{o3})} \right] l_e \quad (7a)$$

Between radiation shield j and $j+1$

$$Q_{gh} = \left[\frac{\pi \sigma d_{rj} (T_{rj}^4 - T_{ij+1}^4)}{\epsilon_{rj}^{-1} + (\epsilon_{ij+1}^{-1} - 1) d_{rj} / d_{ij+1}} + \frac{2\pi k_{he}^{j+1} (T_{rj} - T_{ij+1})}{\ln(d_{ij+1} / d_{rj})} \right] l_e, \quad (7b)$$

$$j = 1, 2, \dots, n - 1; n \geq 2$$

where n is the total number of radiation shield layers wrapped around the guard heater.

Referring to the Appendix for the radiation exchange between coaxial cylinders of equal length, the heat flow balance between the outermost radiation shield and the helium chamber requires that

$$Q_{gh} = \frac{2\pi l_e k_{he}' (T_m - T_{i4})}{\ln(d_{i4} / d_m)} + Q_m(T_m, T_{i4}, T_{i4}) \quad (7c)$$

The net heat flow to the helium chamber wall of length l_e is given by

$$Q_4 = \frac{2\pi l_e k_{he}' (T_m - T_{i4})}{\ln(d_{i4} / d_m)} - Q_{o4}(T_{o3}, T_{o4}, T_{o4}) \quad (7d)$$

Q_m and Q_{o4} are the inner and outer cylinder radiation heat flow rates given in the Appendix and k_{he}' is the average thermal conductivity of the helium gas filling the space between the outermost heat shield and the inside wall surface of the helium chamber. The thermal resistances in Eq. (7b), of the thin foils (0.025 mm) forming the heat shields (not including the wire screens) have been neglected. The temperature of the j th shield is T_{rj} and the diameter is $d_{rj} = d_{rj-1} + 2d_w$, with d_w being the diameter of the screen wire and $d_{r0} = d_{o3}$ being the outside diameter of the guard heater. $k_{eff}^{(j)}$ is the effective thermal conductivity between the radiation shields j and $j + 1$ accounting for the contribution made by the presence of the screen wires in the helium-filled space between the heat shields.

Radial heat conduction is calculated through the helium chamber wall

$$Q_4 = \frac{2\pi k_4 l_e (T_{i4} - T_{o4})}{\ln(d_{o4}/d_{i4})} \quad (8)$$

where Q_4 is given either by Eq. (6b) when heat shields are not used or (7d) when they are used.

Heat exchange within the enclosure between the walls of the helium and vacuum chambers takes place entirely by radiation. The formulation in the Appendix with the cylinder length l_e is used as an approximation. The background radiation is assumed to be due to the stainless steel vacuum chamber walls at a temperature close to that of room air. The net heat flow leaving the outer surface of the helium chamber is given by

$$Q_4 = Q_{o4}(T_{o4}, T_{i5}, T_{air}) \quad (9)$$

The heat flow entering the vacuum chamber wall at the inner surface is

$$Q_4 = Q_{i5}(T_{o4}, T_{i5}, T_{air})$$

Assuming only radial heat flow, this is transferred by conduction across the thickness of the solid wall. Thus

$$Q_{i5}(T_{o4}, T_{i5}, T_{air}) = \frac{2\pi k_5 l_e (T_{i5} - T_{o5})}{\ln(d_{o5}/d_{i5})} \quad (10)$$

Since the same heat must be transferred from the vacuum chamber wall to the room air by convection and to the surrounding walls of the room by radiation

$$Q_{i5}(T_{o4}, T_{i5}, T_{air}) = \pi d_{o5} l_e [\sigma \epsilon_{o5} (T_{o5}^4 - T_w^4) + h_{o5} (T_{o5} - T_{air})] \quad (11)$$

In Eq. (11), the average heat transfer coefficient of free convection h_{o5} over the outer surface of the vacuum chamber was calculated from the multi-valued, two-constant correlation formula suggested by Morgan (1975). The vacuum chamber is treated as a horizontal cylinder for a conservative estimate.

Temperature mismatch between the primary and guard heaters arises both in a random fashion from uncertainties associated with temperature measurement itself and also in a

prescriptive manner necessitated for guard heating control. Radial heat flow by radiation exchange between the two heaters depends mostly on their temperatures and is rather insensitive to the size of the separation gap between them, within modest limits. Once the size of the primary heater has been determined from Fig. 3, it is of advantage to use a guard heater with a diameter large enough to significantly reduce the radial heat flow by conduction through the helium gas. With the heaters operating around 1900 K, a 10-mm gap between the niobium cylinders will reduce the heat transfer by conduction to roughly 30 percent of that by radiation. With the size of the primary heater determined, the component dimensions of the guard heater are shown in Table III.

Table III. Inside diameters of heater unit components.

Primary header, d_{12}	42.24 ⁺ (42.64 [*])mm
Small Nb cylinder	49.39 mm
Large Nb cylinder	70.39 mm
Guard heater, d_{13}	75.39 mm
Helium chamber, d_{14}	20.3 cm
Vacuum chamber, d_{15}	91.4 cm

+ Untreated heat pipe evaporator surface.

* Arc-textured heat pipe evaporator surface.

The solutions obtained from Eqs. (5) to (11) are shown in Fig. 6. They are given in terms of the number of niobium heat shields employed versus the guard heater power output. Also shown in Fig. 6 is the corresponding temperature of the helium chamber

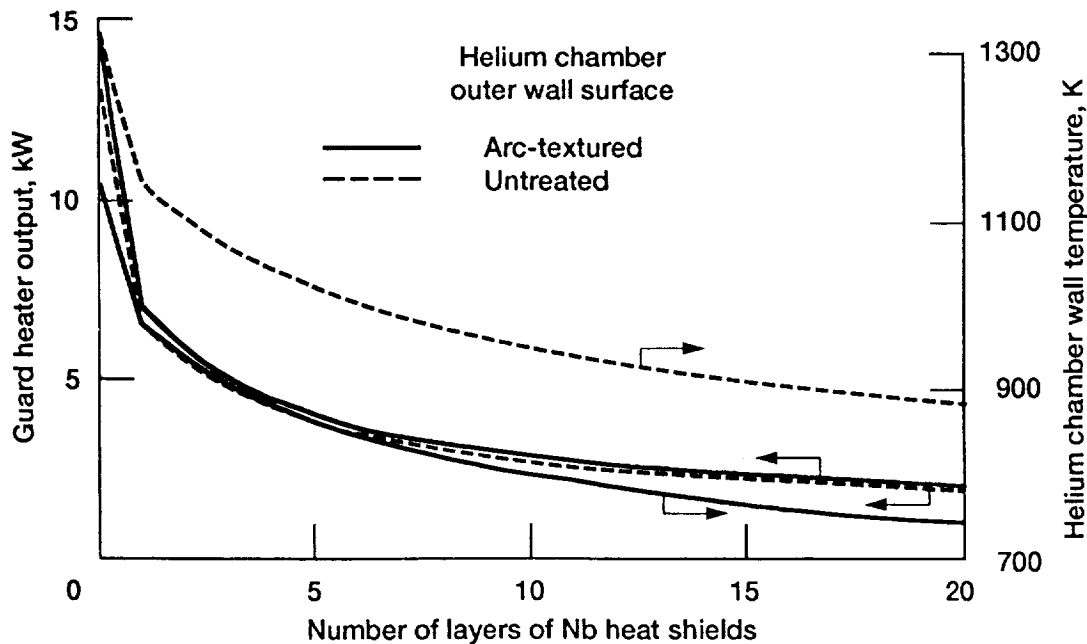


Figure 6.—Guard heater power output and helium chamber wall temperature versus number of niobium shields.

outer surface. It should be noted that an inside guard heater surface temperature of $T_{13} = 1900$ K and room air and surrounding wall temperatures of 298 K were assumed. The various component dimensions used in this calculation are listed in Table III and the component thicknesses in Table II. Two cases are presented in Fig. 6. A case with arc-texturing of the outer surface of the stainless steel wall of the helium chamber is shown along with the same case with that surface untreated. Arc-texturing reduces the wall temperature in all cases over the untreated case. For design purposes the stainless steel helium chamber wall temperature must be kept below 1000 K to maintain the structural integrity of the material. However, reducing the wall temperature of the helium chamber causes the outward radial heat flow from the guard heater to increase. Therefore, it is desired to design the heater assembly to operate with the helium chamber at the highest possible temperature to reduce power requirements for the guard heater. Figure 6 shows that heat shielding alone can keep the temperature of the stainless steel wall of the helium chamber below 1000 K. Arc-texturing reduces the helium chamber temperature but is not needed if the appropriate number of heat shields are used. It would be possible to reduce guard heater power requirements and eliminate the need for heat shields outside the guard heater by operating the helium chamber at temperatures higher than 1000 K. Fabricating the helium chamber of Niobium was considered. This would significantly increase the maximum operating temperature of the helium chamber, however the cost was prohibitive.

Calorimeter Assembly

The primary and guard calorimeters are shown in Fig. 1. A thin tubing of soft copper is continuously wound and solder-jointed at a constant pitch around a base cylinder which has a length equal to that of the heat pipe's condenser section. A thin cylindrical outer shell is mounted over the tube windings so that a transversely bounded annular region is formed. The flow of the coolant is confined to the region between the neighboring windings and the flow path forms a continuous spiral around the base cylinder within the annulus. Table IV lists the basic specifications common to both calorimeters.

Table IV.—Calorimeter specifications.

Coolant:	
Aqueous Ethylene Glycol, percent by volume	50
Inlet temperature, K	298
Temperature rise, K	30
Material	Copper
Axial length, m	0.5
Outside diameter of winding tube, mm	4.76
Wall thickness of base cylinder, mm	2.38

The cutaway schematic of a representative section of the primary calorimeter is shown in Fig. 7. Heat is transferred from the condensing vapor inside the heat pipe to the cooling fluid flowing spirally around the base cylinder. The following equations can model radial heat flow for the configuration at steady state operating conditions

-  Primary coolant flow
-  Secondary coolant flow

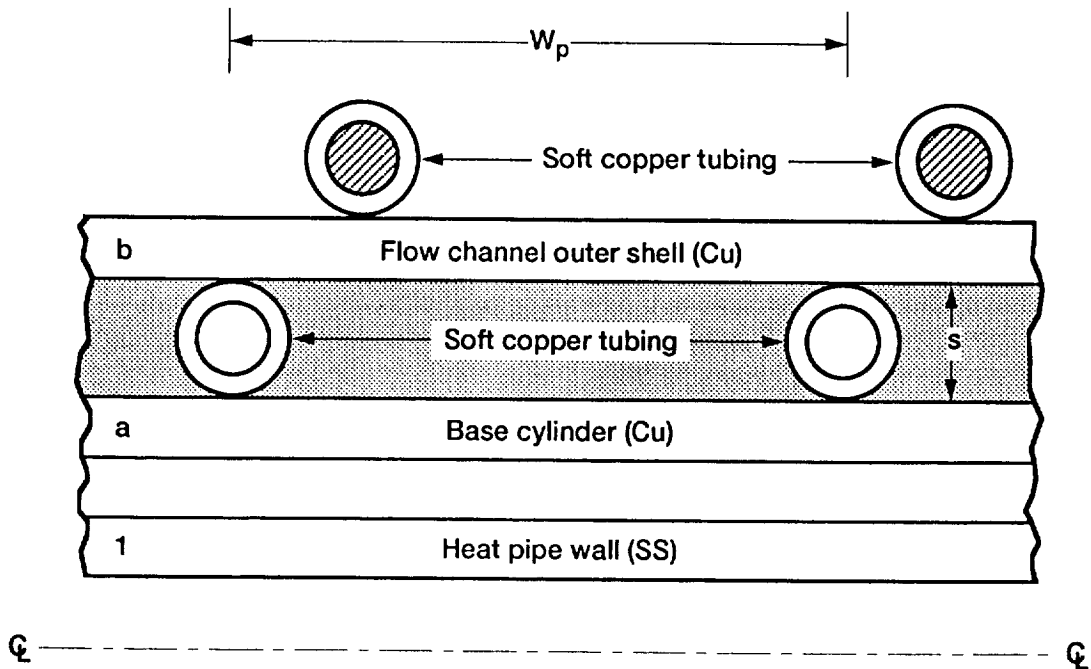


Figure 7.—Schematic of primary calorimeter; component labels: 1, a, and b.

Heat flow through pipe wall

$$Q_c = 2\pi k_1 l_c (T_{i1} - T_{o1}) / \ln \frac{d_{o1}}{d_{i1}} \quad (12)$$

Heat flow through helium gap

$$Q_c = \left[\frac{\pi \sigma d_{o1} (T_{o1}^4 - T_{ia}^4)}{\epsilon_{o1}^{-1} + (\epsilon_{ia}^{-1} - 1) d_{o1} / d_{ia}} + \frac{2\pi k_{he} (T_{o1} - T_{ia})}{\ln(d_{ia} / d_{o1})} \right] l_c \quad (13)$$

Heat flow through base cylinder

$$Q_c = 2\pi k_{ac} l_c (T_{ia} - T_{or}) / \ln \frac{d_{oa}}{d_{ia}} \quad (14)$$

Heat flow into coolant

$$Q_c = \pi d_{oa} l_c h_f (T_{oa} - \bar{T}_b) \quad (15)$$

where T_b is the mean fluid bulk temperature between the inlet and the outlet of the coolant flow channel. h_f is the coolant flow heat transfer coefficient.

A number of quantities pertinent to the description of the coolant flow are calculated from the following relations:

Coolant flow channel length

$$l_f = \left[\pi^2 d_{oa}^2 (l_c / w_p - 1)^2 + l_c^2 \right]^{1/2}$$

Coolant flow channel width

$$w_f = w_p \cos \left[\sin^{-1} (l_c / l_f) \right]$$

Coolant flow area

$$A_f = w_f s - \pi s^2 / 4$$

Coolant flow hydraulic diameter

$$D_h = 4A_f / (\pi s + 2w_f)$$

Coolant flow average velocity

$$U_f = Q_c / (\rho c A_f \Delta T_b)$$

Coolant flow channel Reynolds number

$$Re = \rho U_f D_h / \mu$$

Coolant flow Nusselt number

$$Nu = h_{oa} k / D_h$$

Coolant flow Prandtl number

$$Pr = \mu c / k$$

For aqueous ethylene glycol obtained by mixing equal volumes of the pure components, these bulk properties as functions of temperature can be calculated from the data given by Mills (1992). Turbulent flow is assumed. To account for the influence of curvature, the friction factor, f , of the spiral flow around the base cylinder is obtained by using the correlation (Schlichting 1968)

$$f = f_o \left[1 + 0.075 Re^{1/4} \left(\frac{s'}{d_{oa}} \right)^{1/2} \right] \quad (16)$$

where s' is either the width of the flow gap in the calorimeter as shown in Fig. 7 or replaced by D_h , whichever is larger, for a more conservative estimate than the exact expression.

$$f_o = (0.79 \ln Re - 1.64)^{-2} \quad (17)$$

Equation (17) is the friction factor for turbulent flow in a smooth straight pipe. The pressure drop along the flow channel between the inlet and outlet is calculated by the expression

$$\Delta p = f_l f_f \frac{\rho U_f^2}{2D_h} \quad (18)$$

The average heat transfer coefficient for the coolant flow heat transfer was conservatively computed for design purposes on the basis of the correlation proposed by Gnielinski (1976).

$$Nu = \frac{(f/8)(Re - 1000)Pr}{1 + 12.7(f/8)^{1/2}(Pr^{2/3} - 1)} \quad (19)$$

The dimensions of the primary calorimeter and the required pressure drop of the coolant flow were calculated using the equations above. The thermal resistance between the condensing vapor and the inside surface of the heat pipe containment envelope was assumed negligible. The heat flowing out of the heat pipe in the condenser section, Q_c , was specified along with the coolant temperature rise, ΔT_b . By using the quantities specified in Table IV, these equations uniquely determine the axial pitch distance of tube windings, w_p , the inner diameter of the base tube, d_{ia} , and the required coolant pressure drop, Δp . The solutions are shown in Fig. 8. The primary calorimeter inside diameter is

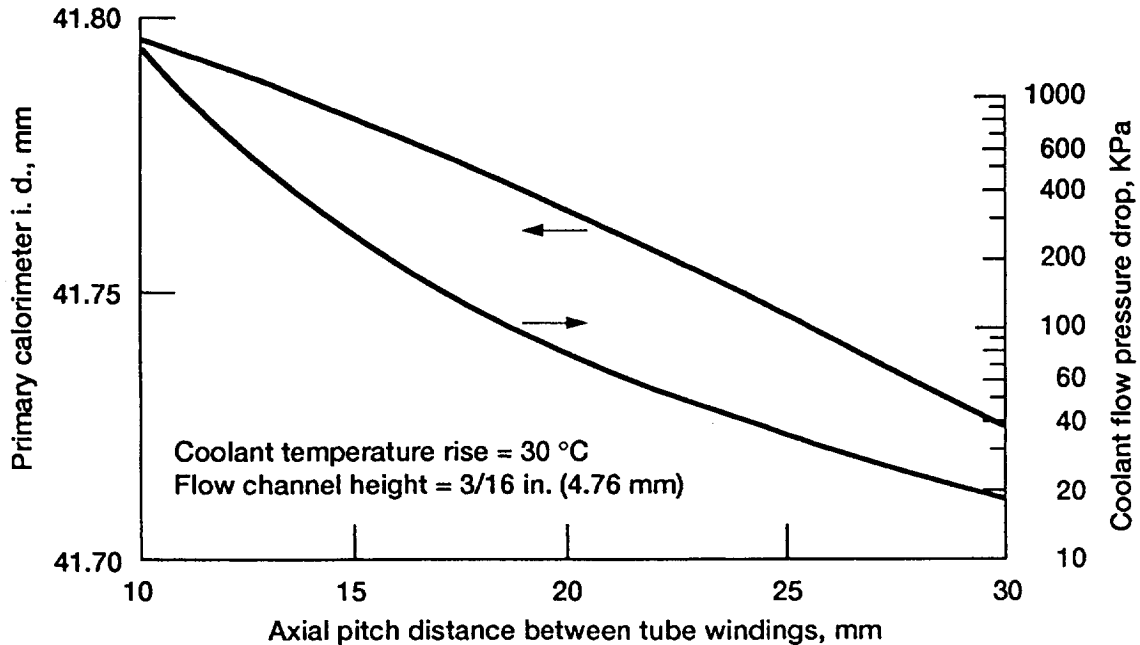


Figure 8.—Primary calorimeter requirements at heat pipe design operating conditions; coolant fluid: aqueous ethylene glycol, 50-50 by volume.

plotted against the axial pitch distance between tube windings. Also shown is the corresponding pressure drop of the coolant flow. These results were generated for the design case of a condenser heat load of 20 kW, and a coolant mass flow rate which resulted in a coolant temperature rise of 30 K between inlet and outlet sections. Decreasing the winding pitch distance results in a higher coolant flow velocity and thus a larger pressure drop and heat transfer coefficient. This produced little change in the primary calorimeter inner diameter which increases from 41.71 to 41.79 mm for a two-fold increase in coolant flow velocity. The outside diameter of the baseline heat pipe becomes 40.66 mm at the design

temperature because of thermal expansion. A gas gap of 0.5 mm was chosen between the primary calorimeter and the heat pipe. So a helium gap larger than 0.5 mm exists between the heat pipe and the primary calorimeter at heat pipe operating temperatures below 1000 K because of thermal expansion. From this analysis it was found that the selection of the coolant flow channel width can be made on the basis of pressure drop requirements.

Adiabatic Section

It is of interest to determine the heat losses from the "adiabatic section" of the heat pipe. The procedure outline for calculating the heat transfer for the guard heater was modified for this purpose. This procedure accounts for heat transfer by conduction, radiation, and free convection. Stainless steel heat shields are used to reduce heat flow out of this section of the heat pipe. The calculated heat loss rate of the adiabatic section is expressed as a percentage of the evaporator heat rate at heat pipe operating temperatures of 500 and 1000 K. This percentage is plotted against the number of heat shields which surround the adiabatic section in Fig. 9. The heat loss can be reduced slightly by adding heat shields. The heat loss from the "adiabatic section" of the heat pipe has been shown to be rather small with respect to the total heat transported by the heat pipe.

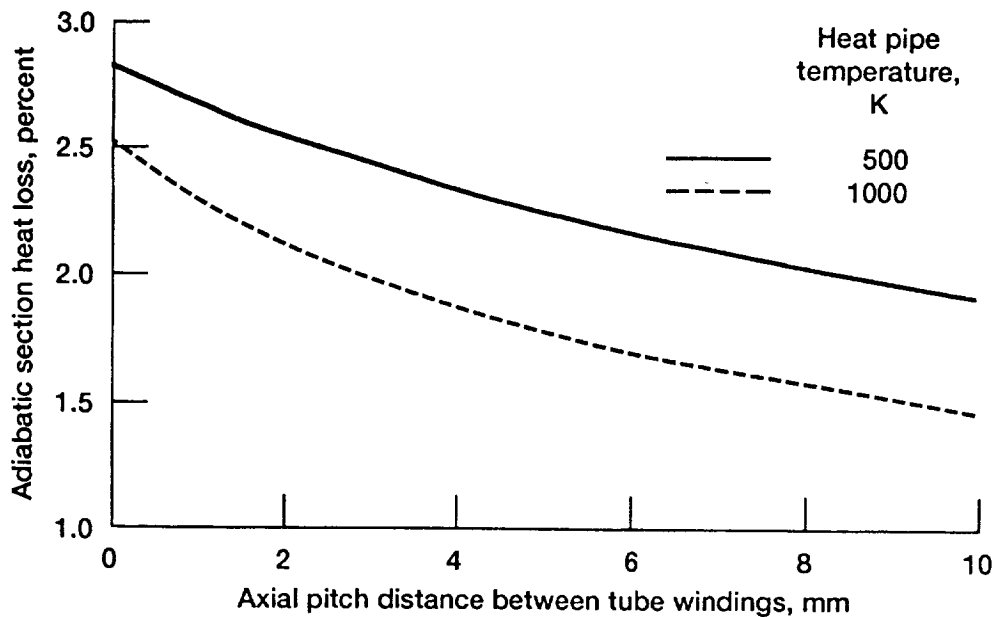


Figure 9.—Rate of heat loss from the adiabatic section as a percentage of the heat transport rate of the baseline heat pipe.

OFF DESIGN CONDITIONS

It is desirable to predict how the temperatures and heat flows of the apparatus vary at heat loads less than $Q = 20$ kW. Some of these results are shown in Fig. 10 for a baseline design heat pipe with an untreated evaporator surface, 20-mm calorimeter winding pitch and a coolant flow of 176 ml/s. The heat transported by the heat pipe is plotted against the heat pipe operating temperature, also shown is the primary heater operating

temperature versus the heat pipe operating temperature. The heat pipe operating temperature increases almost linearly with primary heater temperature. The slope of the line for heat load transported by the heat pipe increases as operating temperature of the heat pipe increases. This is a result of radiation heat transfer becoming more significant versus conduction as temperatures increase.

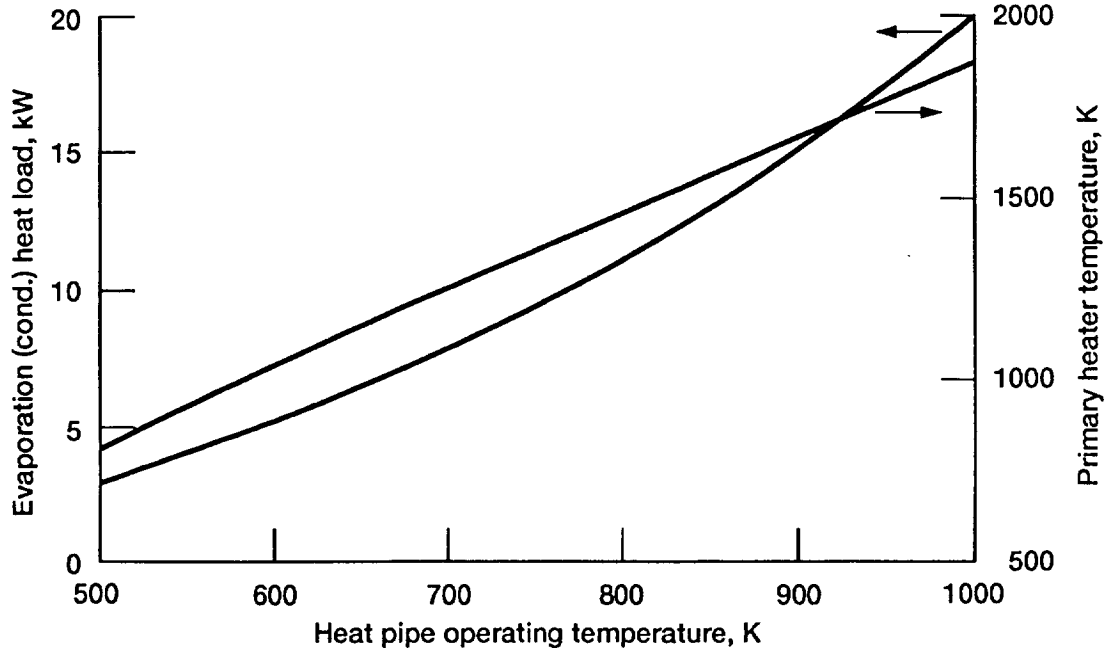


Figure 10.—Heat pipe heat load and primary heater temperature versus heat pipe operating temperature.

CONCLUSION

A heat pipe test apparatus has been designed which has the capability of providing heat loads of up to 20 kW for heat pipe code validation purposes. The test apparatus will be enclosed in a helium gas atmosphere which enhances heat transfer and reduces heater operating temperature. Guarded heating and cooling will be employed to measure data accurately. Two methods of preventing heat pipe destruction upon dry-out have been mentioned.

ACKNOWLEDGMENTS

This work was carried out at the NASA Lewis Research Center and is supported under the NASA Base Research and Technology program. The authors wish to acknowledge Timothy Marks of Oregon State University, Jim Zacony, Miles Dustin, and Leonard Tower of Sverdrup Technology, Incorporated for their contributions to this effort.

NOMENCLATURE

A	area, m^2
c	specific heat, J/kgK
d	diameter of concentric components, m
D_h	hydraulic diameter of coolant transverse flow area, m
f	friction factor
h	heat transfer coefficient, W/m^2K
k	mean thermal conductivity, W/mK
l	length, m
Nu	Nusselt number
P	pressure, N/m^2
Pr	Prandtl number
Q	power output, W
$Q_i(T_i, T_j, T_k)$	net radiation leaving surface i in a three-surface enclosure, W
Re	Reynolds number
s	height of coolant flow channel, m
T	temperature, K
T_b	coolant temperature, K
U	velocity, m/s
w	width of coolant transverse flow area, m
w_p	axial pitch distance between tube windings, m
δ	thickness, m
ϵ	hemispherical emissivity
σ	Stefan-Boltzman constant, W/m^2K^4

ρ density, kg/m³

μ viscosity, kg/ms

Subscripts and Superscripts

a calorimeter base cylinder

b calorimeter outer shell

j component identification

ij refers to inside surface of component with label j

oj refers to outside surface of component having label j

rj refers to heat shield having label j

r heat shields

f coolant transverse flow

c heat pipe condenser section

ph primary heater

e evaporator section

gh guard heater

eff effective

w screen wire

he helium

/ average

REFERENCES

- Banks, B.A., Rutledge, S.K., Mirtich, M.J., Behrend, T., Hote, D., Kussmaul, M., Barry, J., Stidham, C., Stuber, T., and DiFilippo, F., 1988, "Arc-Textured Metal Surfaces for High Thermal Emittance Space Radiators," NASA TM-100894.
- Chang, W.S., 1990, "Porosity and Effective Thermal Conductivity of Wire Screens," Journal of Heat Transfer, Vol. 112, No. 1, pp. 5-9.

- Gnielinski, V., 1976, "New Equations for Heat and Mass Transfer in Turbulent Pipe and Channel Flow," *International Chemical Engineering*, Vol. 16, No. 2, pp. 359-368.
- Incorpera, F.P., and DeWitt, D.P., 1990, Fundamentals of Heat and Mass Transfer, Third ed., Wiley, New York, p. 563.
- Mills, A.F., 1992, Heat Transfer, Irwin, Inc., Homewood, IL, p. 834.
- Morgan, V.T., 1975, "The Overall Convective Heat Transfer from Smooth Circular Cylinders," Advances in Heat Transfer, T.F. Irvine & J.P. Hartnett, eds., Academic Press, New York, Vol. 11, pp. 199-264.
- Schlichting, H., 1968, Boundary-Layer Theory, J. Kestin, transl., McGraw-Hill, New York, p. 589.
- Siegel, R. and Howell, J.R., 1981, Thermal Radiation Heat Transfer, 2nd. ed, Hemisphere Publ., Washington, DC, p. 828.
- Touloukian, Y.S. and Ho, C.Y. eds., 1972, Thermophysical Properties of Matter, Plenum Press, New York.
- Union Carbide Coating Service Corp., 1990 Borallloy (Trademark): Pyrolytic Boron Nitride CP-4779, Rev. 3, M 8/90.

APPENDIX A—RADIATION HEAT EXCHANGE IN AN ENCLOSURE BETWEEN TWO CONCENTRIC CYLINDERS OF EQUAL LENGTH

The common length of the cylinders is denoted by l . the inner cylinder is designated by an index i , the outer cylinder by j , and the imaginary surfaces of the open-ended annulus by k . The radiation balance equations for the determination of the total radiosities of the surfaces are:

$$\left(\frac{\epsilon_i}{1 - \epsilon_i} + F_{ij} + F_{ik} \right) J_i - F_{ij} J_j - F_{ik} J_k = \frac{\sigma \epsilon_i T_i^4}{1 - \epsilon_i} \quad (\text{A-1})$$

$$-F_{ji} J_i + \left(\frac{\epsilon_j}{1 - \epsilon_j} + F_{ji} + F_{jk} \right) J_j - F_{jk} J_k = \frac{\sigma \epsilon_j T_j^4}{1 - \epsilon_j} \quad (\text{A-2})$$

$$-F_{ki} J_i - F_{kj} J_j + \left(\frac{\epsilon_k}{1 - \epsilon_k} + F_{ki} + F_{kj} \right) J_k = \frac{\sigma \epsilon_k T_k^4}{1 - \epsilon_k} \quad (\text{A-3})$$

The net rate of radiation heat flow from the surfaces is given by:

$$Q_i(T_i, T_j, T_k) = \frac{\epsilon_i \pi d_i l}{1 - \epsilon_i} (\sigma T_i^4 - J_i) \quad (\text{A-4})$$

$$Q_j(T_i, T_j, T_k) = \frac{\epsilon_j \pi d_j l}{1 - \epsilon_j} (\sigma T_j^4 - J_j) \quad (\text{A-5})$$

$$Q_k(T_i, T_j, T_k) = \frac{\epsilon_k \pi l (d_j^2 - d_i^2)}{4(1 - \epsilon_k)} (\sigma T_k^4 - J_k) \quad (\text{A-6})$$

The configuration factors viewed from the outer cylinder with respect to the inner cylinder and with respect to itself are:

$$F_{ji} = \frac{1}{R} - \frac{1}{\pi R} \left\{ \cos^{-1} \frac{V}{U} - \frac{1}{2L} \left[\sqrt{(U+2)^2 - 4R^2} \cos^{-1} \frac{V}{RU} + V \sin^{-1} \frac{1}{R} - \frac{\pi U}{2} \right] \right\}$$

$$F_{jj} = 1 - \frac{1}{R} + \frac{2}{\pi R} \tan^{-1} \frac{2\sqrt{R^2 - 1}}{L} - \frac{1}{2\pi R} \left[\frac{\sqrt{4R^2 + L^2}}{L} \sin^{-1} \frac{4(R^2 - 1) + (L^2/R^2)(R^2 - 2)}{L^2 + 4(R^2 - 1)} \right. \\ \left. \sin^{-1} \frac{R^2 - 2}{R^2} + \frac{\pi}{2} \left(\frac{\sqrt{4R^2 + L^2}}{L} - 1 \right) \right]$$

where

$$R = \frac{d_j}{d_i}, \quad L = \frac{l}{d_i}, \quad U = L^2 + R^2 - 1, \quad V = L^2 - R^2 + 1$$

From the reciprocity relation

$$F_{ij} = \left(\frac{d_j}{d_i} \right) F_{ji};$$

Since for the inner cylinder, $F_{ii}=0$, thus

$$F_{ik} = 1 - F_{ij}$$

Consequently:

$$F_{jk} = 1 - F_{ji} - F_{jj}$$

$$F_{ki} = \frac{4d_i F_{ik}}{(d_j^2 - d_i^2)}$$

$$F_{kj} = \frac{4d_j F_{jk}}{(d_j^2 - d_i^2)}$$

REPORT DOCUMENTATION PAGE

Form Approved
OMB No. 0704-0188

Public reporting burden for this collection of information is estimated to average 1 hour per response, including the time for reviewing instructions, searching existing data sources, gathering and maintaining the data needed, and completing and reviewing the collection of information. Send comments regarding this burden estimate or any other aspect of this collection of information, including suggestions for reducing this burden, to Washington Headquarters Services, Directorate for Information Operations and Reports, 1215 Jefferson Davis Highway, Suite 1204, Arlington, VA 22202-4302, and to the Office of Management and Budget, Paperwork Reduction Project (0704-0188), Washington, DC 20503.

1. AGENCY USE ONLY (Leave blank)	2. REPORT DATE July 1992	3. REPORT TYPE AND DATES COVERED Technical Memorandum	
4. TITLE AND SUBTITLE Design Characteristics of a Heat Pipe Test Chamber		5. FUNDING NUMBERS WU-506-41-51	
6. AUTHOR(S) Karl W. Baker, J. Hoon Jang, and Juin S. Yu			
7. PERFORMING ORGANIZATION NAME(S) AND ADDRESS(ES) National Aeronautics and Space Administration Lewis Research Center Cleveland, Ohio 44135-3191		8. PERFORMING ORGANIZATION REPORT NUMBER E-7142	
9. SPONSORING/MONITORING AGENCY NAMES(S) AND ADDRESS(ES) National Aeronautics and Space Administration Washington, D.C. 20546-0001		10. SPONSORING/MONITORING AGENCY REPORT NUMBER NASA TM-105737	
11. SUPPLEMENTARY NOTES Prepared for the First International Conference on Aerospace Heat Exchanger Technology, cosponsored by the ASME and IAAA, Palo Alto, California, February 15-17, 1993. Karl W. Baker, NASA Lewis Research Center, Cleveland, Ohio; J. Hoon Jang, Sverdrup Technology, Inc., Lewis Research Center Group, 2001 Aerospace Parkway, Brook Park, Ohio 44142. Juin S. Yu, West Virginia Institute of Technology, Montgomery, West Virginia 25136. Responsible person, Karl W. Baker, (216) 433-6162.			
12a. DISTRIBUTION/AVAILABILITY STATEMENT Unclassified - Unlimited Subject Category 44		12b. DISTRIBUTION CODE	
13. ABSTRACT (Maximum 200 words) The Lewis Research Center of the National Aeronautics and Space Administration has designed a heat pipe test facility which will be used to provide data for validating heat pipe computer codes. A heat pipe test chamber that uses helium gas for enhancing heat transfer has been investigated. The conceptual design employs the technique of guarded heating and guarded cooling to facilitate accurate measurements of heat transfer rates to the evaporator and from the condenser. The design parameters are selected for a baseline heat pipe made of stainless steel with an inner diameter of 38.10 mm and a wall thickness of 1.016 mm. The heat pipe operates at a design temperature of 1000 K with an evaporator radial heat flux of 53 W/cm ² .			
14. SUBJECT TERMS Heat pipe; High temperature; Design		15. NUMBER OF PAGES 26	
		16. PRICE CODE A03	
17. SECURITY CLASSIFICATION OF REPORT Unclassified	18. SECURITY CLASSIFICATION OF THIS PAGE Unclassified	19. SECURITY CLASSIFICATION OF ABSTRACT Unclassified	20. LIMITATION OF ABSTRACT

